

# Preliminary results in development of an object-based image analysis method for earthquake damage assessment

T. Thuy Vu<sup>1</sup>, Masashi Matsuoka<sup>1</sup>, Fumio Yamazaki<sup>2</sup>

<sup>1</sup>Earthquake Disaster Mitigation Research Center (EDM), National Institute for Earth Science and Disaster Prevention (NIED), JAPAN

1-5-2 Kaigandori, Wakinohama, Chuo-ku, Kobe 651-0073

Email: [thuyvu@edm.bosai.go.jp](mailto:thuyvu@edm.bosai.go.jp) and [matsuoka@edm.bosai.go.jp](mailto:matsuoka@edm.bosai.go.jp)

<sup>2</sup>Department of Urban Environment Systems, Faculty of Engineering, Chiba University, JAPAN

1-33 Yayoi-cho, Inage-ku, Chiba 263-8522

Email: [yamazaki@tu.chiba-u.ac.jp](mailto:yamazaki@tu.chiba-u.ac.jp)

## ABSTRACT

The commercialization of very high resolution (VHR) satellite images such as QuickBird and IKONOS has expanded the applications of remote sensing techniques, especially in the field of disaster assessment. However, development of VHR processing methods is far behind the application progress. For instance, visual interpretation earthquake damaged buildings is still the most reliable method. Providing a highly detailed scene, a VHR satellite image requires much more complicated processing. Since the conventional pixel-based methods cannot provide the reliable analyzed results, a new object-based method which is built on area morphology is proposed. This paper presents the preliminary development of this newly proposed method. The promising results infer that the method can be widely employed in damage detection of building inventory updating.

## 1. INTRODUCTION

Recent catastrophes have been observed and captured by various remote sensors on different platforms like space-borne or airborne. It triggers a great employment of remote sensing techniques in post-disaster response. The review here focuses on the employment of remote sensing in earthquake damage assessment only. Many researches and implementations have been carried out after several recent big earthquakes such as the 1995 Kobe, Japan earthquake (Matsuoka and Yamazaki 1999), the 1999 Kocaeli, Turkey earthquake (Eguchi et al. 2000, Estrada et al. 2000), the 2001 Gujarat, India earthquake (Mitomi et al. 2001, Saito et al. 2004), the 2003 Bam, Iran earthquake (Vu et al. 2005, Yamazaki et al. 2005). Either optical or radar, images at different resolutions have been used. The availability of higher resolution images these days allows the interpretation of damage scale of each building block or even each individual building rather than damage distribution and damage extent. Both visual and automated interpretations are used to derive the damage information from remotely sensed images.

At the lowest level of processing, image processing deals with pixel. Each pixel possesses

the grey value which represents the spectral reflectance at its location. Based on that, a vast amount of algorithms called pixel-based was developed. Texture-based algorithms are the higher level of processing which analyze different kinds of relationship among the neighbors of each pixel. These two types of processing have been successfully used with coarse resolution images like Landsat and ERS (Matsuoka and Yamazaki, 1999; Eguchi et al., 2000; Estrada et al., 2000). The reason is that coarse image does not provide the detailed information. A pixel itself might be a mixture of different objects. Therefore, pixel or texture information is the reasonable cue for the detection and extraction of damage extent and distribution. Airborne-based images and very high resolution (VHR) satellite images such as QuickBird and IKONOS, which provide highly detailed information, require much more complicated processing. Those pixel-based and texture-based methods developed could be used with airborne-based images (Mitomi et al. 2001) and VHR satellite images (Vu et al. 2005). However, it was unable to exploit all possessed information in a high resolution image. The visual interpretation, which obviously is time-consuming and requires the experienced interpreters, has been more reliable method (Yamazaki et al. 2005). To

automate the interpretation, object-based image processing should be developed.

Objects presented on an image possess the scale property. Exploitation of scale in image processing, in fact, mimics the human perception. Human perception ignores the details and groups the pixels into an object at a specific scale of observation. Linear scale-space has been well-developed in feature extraction and visualization (Lindeberg, 1993). To overcome the distortion problem at coarser scale by the linear scale-space, which generates the difficulty in linking across the scale-space, non-linear scale space is proposed. Non-linear scale space keeps the main properties of a scale-space like luminance conservation, geometry, or morphology (Petrovic et al. 2004). Generally, it performs a partition of an image into isolevel sets at each scale and links them with the closet one in the next scale. The proposed method presented in this paper employs area morphology (Vincent 1992) to construct the nonlinear scale-space. Its theory will be presented in Section 2. Several preliminary developments for assistance the visual interpretation, detection of damaged buildings, and building extraction are reported in Section 3. Summary and discussion of further developments will be in Section 4.

## 2. SCALE-SPACE BASED ON AREA MORPHOLOGY

Vincent (1992) defines that area opening filtering removes the components with area smaller than a parameter  $s$  from a binary image. Similarly, area closing filtering fills the holes with area smaller than a parameter  $s$ . The binary area opening is defined as follows; Let set  $X$  is a subset of set  $M \subseteq R^2$  and  $\{X_i\}$  is all the connected components of  $X$ . The area opening of parameter  $s$  ( $s \geq 0$ ) of  $X$ , represented as  $\gamma_s^a(X)$ , is the union of the connected components of  $X$  with area greater than  $s$ . The area closing of parameter  $s$  ( $s \geq 0$ ) of  $X$ , represented as  $\phi_s^a(X)$ , is then defined as area opening of parameter  $s$  on the complement of  $X$  in  $M$ .

Vincent (1992) then extended the definition of binary area opening or closing to grayscale area opening or closing. A grayscale image can be

defined as a mapping  $f : M \rightarrow R$ . The grayscale opening of  $f$  is described as follows. The image  $M$  is firstly threshold with all the possible  $h$  and the binary opening  $\gamma_s^a(T_h(f))$  is found. Subsequently, supremum, i.e. a lowest upper bound, is applied to all the recently found  $\gamma_s^a(T_h(f))$ . It is similarly extended to grayscale closing by duality. Area morphological filtering does not depend on the shape of structural elements as the conventional one. Therefore, it can effectively remove noise and simultaneously retain thin or elongated objects. For simple presentation, area opening/closing means grayscale opening/closing in the rest of this paper.

Applying area opening followed by area closing with a parameter  $s$ , named *AOC* operator, on an image is hence, like flattening this image by parameter  $s$ . This performance segments an image into the flat zones of similar intensity or isolevel sets, in other words. Therefore, a scale-space can be generated by iterative applying *AOC* with increasing  $s$ . The desirable properties of a scale space like fidelity, causality, Euclidean invariance, are hold by *AOC* scale-space (Acton and Mukherjee, 2000). Figure 1 demonstrates three scales  $s = 9, 300, \text{ and } 1200$  of the *AOC* performance on a grayscale image. The small details disappear on the coarse scales and an object can be formed at a specific scale depending on its size. For instance, a small house at the bottom-left of the image was fragmented into two objects on scale  $s = 9$ , it was totally formed on scale  $s = 300$  and disappeared on scale  $s = 1200$ .

Theoretically, the scale-space is generated by an infinite number of scales. For the discrete dimension of an image, the number of scales increases one each as a window (area) size increases from one pixel to an image size. However, it is time-consuming to concern all the area values. Practically, a scene contains a limited number of sizes. Horizontal and vertical granulometry analyses (Vincent, 1994) are carried out to find the potential patterns contained in an image. The local maximum found in horizontal and vertical dimensions can be used to compute the possible areas of objects in the image.

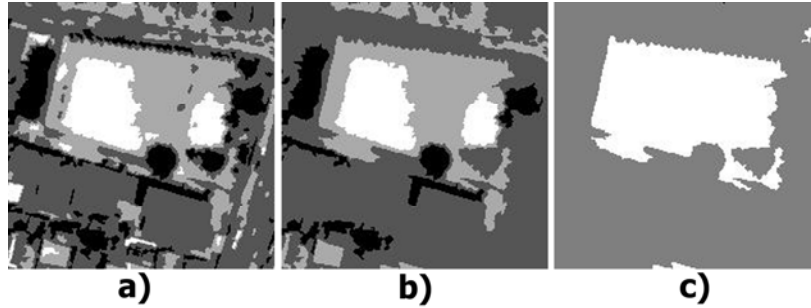


Figure 1. Demonstration of AOC images on scales a)  $s = 9$ , b)  $s = 300$ , and c)  $s = 1200$ .

Across the scale space from a coarse scale to the finer ones, an object is created and split. To extract the objects from the scale-space of a grayscale image, the linking trees of objects must be formed across the scale space. On each scale, an object might have its parent on next coarser scale and its children on next finer scale. The similarity of object's intensity is the criterion to determine the hierarchical relationship. If an object's intensity is much different from that of the big object which it falls into, the scale on which it is created is the root of the linking tree. Subsequently, an object can be extracted at its root scale along with its associated linking tree.

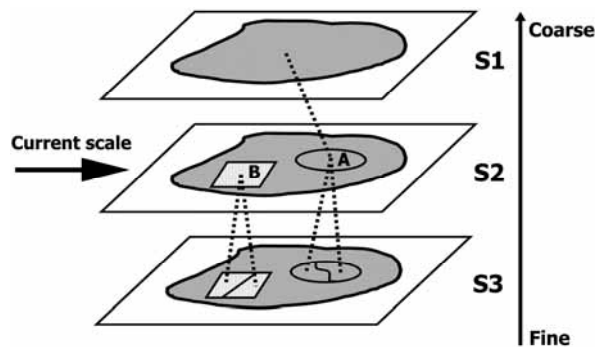


Figure 2. Objects linking across the scale space.

Figure 2 demonstrates the idea of linking object across the scale space. Let assume that we are considering three-scale space with  $S1$  is the coarsest and  $S3$  is the finest one. On the current scale  $S2$ , there are two newly created objects named  $A$  and  $B$ . While  $A$  has similar intensity to the bigger one at scale  $S1$ ,  $B$  has different intensity. As a result,  $B$  can be extracted at this scale  $S2$  with its two-level tree and  $A$  is associated with its father

at  $S1$  and two children at  $S3$  to form a three-level tree.

### 3. PRELIMINARY DEVELOPMENT

The brief description of area morphology scale space in Section 2 mentioned the operation on grayscale image only. Practically, multi-spectral images are being used. Our recent development is adopting the idea in processing the multi-spectral VHR satellite images such as QuickBird. The proposed method is promising for image classification, segmentation or feature extraction in general. Focusing on earthquake damage assessment, we are developing and implementing the idea into three dedicated tools for assistance of visual interpretation, detection of damaged buildings, and extraction of buildings for developing building inventory database.

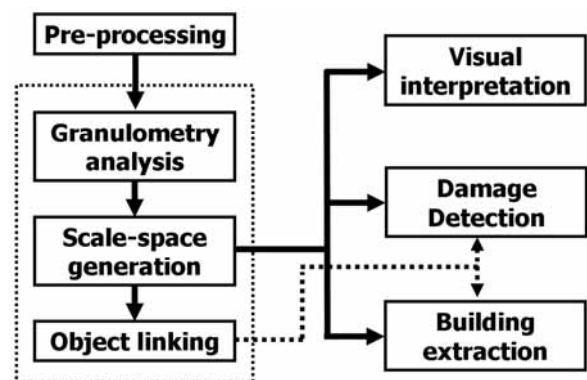


Figure 3. Block diagram of processing.

However, these three tools are sharing the pre-processing and scale-space generation steps (Figure 3). Pre-processing includes the common tools like radiometric correction, geometric

correction, or image sharpening which were well-developed in several remote sensing processing packages. This step utilizes the existing tools in commercial packages. Our developed tools begin at granulometry analysis and scale-space generation as shown in Figure 3. They are built based on the theory presented in Section 2. To facilitate the processing of multi-spectral images, granulometry analysis is carried out on the first component of principal component analysis (PCA). Scale space is separately generated for each spectral band. It can be directly used for assistance of visual interpretation. The object linking is required for building extraction and damage detection. Current developments of visual interpretation, damage detection, and building extraction are reported in the following subsections.

### 3.1. Assist visual interpretation

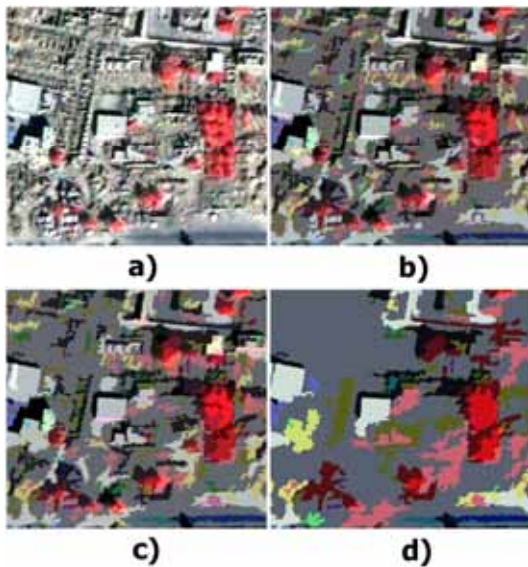


Figure 4. FCC images of an area in Bam: a) original and on scales b)  $s = 50$ , c)  $s = 100$ , d)  $s = 1000$ .

To locate and analyze a feature on an image, human perception tries to group the pixels into one feature by ignoring the details around and inside the feature. In other words, it is like to simplify the information in the neighbor of an analyzed feature. Since scale space presentation of an image mimics that process, we can exploit it to assist the visual interpretation. A small portion of QuickBird scene acquired over Bam, Iran after the earthquake on

December 26, 2003 is used for demonstration. Original image in false-color-composite (FCC) is shown in Figure 4a. Instead of spending time by human simplification, the scale-space generation module opens the image to the scales  $s = 50$ ,  $s = 100$ , and  $s = 1000$  as shown in Figure 4b, 4c and 4d, respectively. Across the scale space from Figure 4b, 4c to 4d, the buildings of increasing sizes can be detected. This process not only helps the interpreter to locate a feature easily but also to extract a feature into a GIS-ready-to-use format in a more automated manner.

### 3.2. Damaged building detection

The research on detection of damaged building is still going on. There are currently two approaches: solely use the post-event image and comparison between the pre-event and the post-event images. The former can avoid the problem of the inexistence of the pre-event image and the difficulties in comparison caused by sensor's look angle, man-made changes, or seasonal changes, etc. To detect the damage, it searches the area of debris based on the edge information. As a result, only damage location can be detected. Even more difficult by using the latter, to derive more damage information, it is preferred. Like any change detection, the chosen approach can be categorized into two types. Two images can be directly compared to fast locate the changes or each of them is separated classified/segmented and the results will be compared. To be also able for feature extraction, extraction of the buildings prior to comparison is chosen.

Firstly, K-mean clustering is employed on each scale to assign the class index to the objects according to their spectral signatures. The K-mean clustered results of the QuickBird image of Bam, Iran on three scales are shown in Figure 5. The above row shows the results on the pre-event image, and the below one shows the ones on the post-event image. The class indexes are then grouped into vegetation, water, shadow, building, etc. This information is stored in a database which will be used in the object linking process.

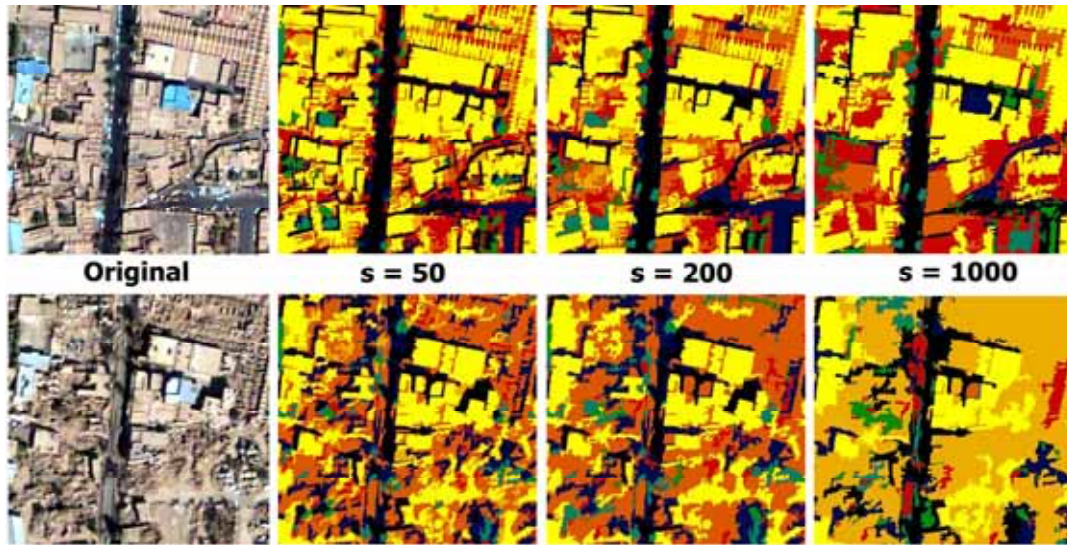


Figure 5. The results of K-mean clustering the spectral signatures on scales  $s = 50$ ,  $s = 200$  and  $s = 1000$ .

There are two possible solutions for further analysis. The first solution employs the object linking module to separately extract the buildings from the pre-event and post-event images prior to the comparison. The second solution detects the changes of the buildings on each scale and the detected changes are linked across the scale-space. Which solution is better is currently considered. The following paragraph describes the process of object linking.

All objects are linked and the relationships are stored in a database. However, focusing on building features, other classes are ignored in the extraction. The linking is started at the finest scale. The attributes of each object are

- SCALE: the current scale it exists,
- ID: the identified number on the current scale,
- AREA: object's area,
- X0, Y0: image coordinates of the starting point of object,
- X, Y: image coordinates of the centroid; this point will be shifted to an arbitrary location inside the object if it is concave object,
- SHAPE: to indicate object is convex or concave,
- SPECTRAL: spectral class,

- SUPERID: the identified number of object's father on next coarser scale, this number equals 0 if the scale is the root of this object.

The criteria to determine the relationship between an object and its potential father are the spectral class. Subsequently, a building can be extracted at its root scale. Figure 6 shows the extracted buildings from the pre-event and post-event images of Bam. Three coarsest scales are used for demonstration. They are combined in Red, Green and Blue channels for scales  $s = 500$ ,  $1000$  and  $2000$ , respectively. Similarly to Figure 5, the above row shows original version and extracted results from the pre-event image and the below row shows the ones from the post-event image. Obviously, less numbers of buildings are retained in the post-event image.

For detailed damage detection, object-based method allows the comparison across the scale space according to the extracted attributes. Probably, totaled collapsed, moderated damaged and non-damaged buildings can be detected. The processing is under developed. To provide an entire figure, extracted buildings are combined across the scale spaces and the areas of damaged buildings can be shown in Figure 7. Color-code of

extracted buildings following the building ID and the scales. Dark blue areas stand for background in Figure 7a, 7b and bright areas on Figure 7c stand for areas of damaged buildings.

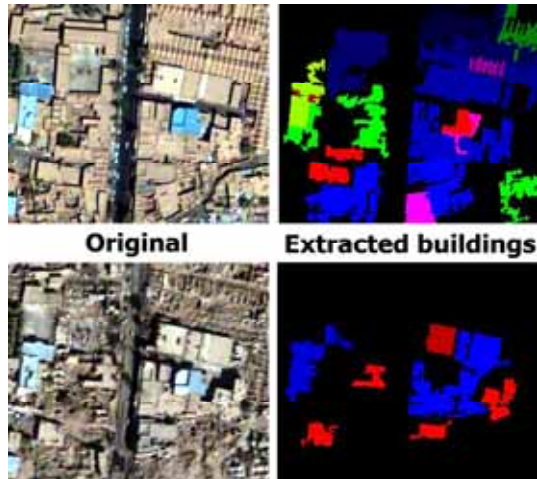


Figure 6. Demonstration of extracted buildings for damage detection. Left: true-color-composite of the pre-event image (above) and the post-event image (below). Right: extracted buildings on scale  $s = 500, 1000, 2000$  on Red, Green, Blue channels.

### 3.3. Building extraction

The presented scheme for damage detection which includes the building extraction in Section 3.2 can be utilized for building extraction in general. The extracted information will be the update for building inventory database. However,

more spectral categories should be concerned and more context information should be retrieved. Because a building is not always a convex or concave polygon, the context information is necessary to combine the extracted parts of a complex structure into one. More works need to be carried out to develop this processing of the building shape. Current development utilizes the feature extraction module described in Section 3.3 to extract different types of buildings in a very dense area. It aims to investigate the capability of the developed module and also the VHR satellite image.

The QuickBird image acquired on June 1<sup>st</sup>, 2004 over Ho Chi Minh City, Vietnam were used for testing. The demonstration in this paper focuses in a small area of downtown (Figure 8). While complex buildings are sparsely distributed in Test A, dense residential area can be observed in Test B. Figures 9 and 10 illustrate the extracted results of big and complex building in Test A area and many small residential areas in Test B. The dark blue is background in these figures. The results showed that big building can be successfully extracted both in Test A and Test B (Figure 9 and Figure 10). Even though the finest scale was 10 pixels, a building whose area is bigger than 10 pixels but spectral reflectance is low contrast compared to the surrounding can not be extracted (Figure 10).

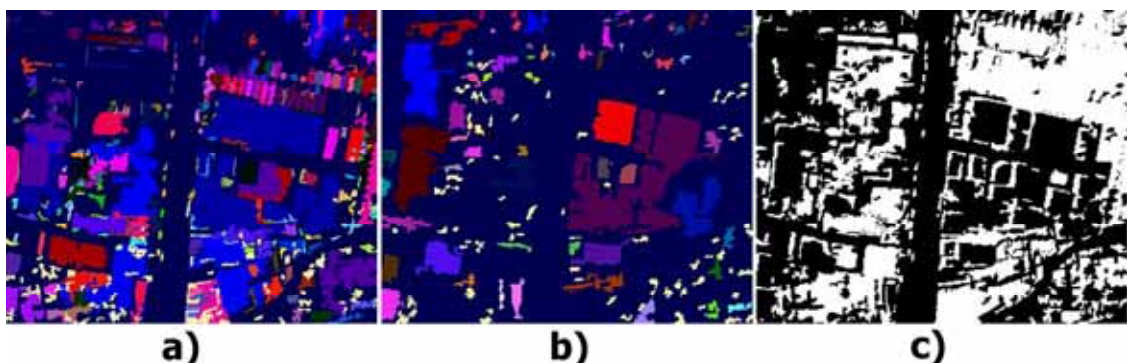


Figure 7. All extracted buildings from the pre-event image (a), the post-event image (b) and areas of damaged buildings (c).



Figure 8. Demonstrated areas in Ho Chi Minh City, Vietnam

#### 4. CONCLUSION

Object-based image analysis based on area morphology is a very promising feature extraction method. It is applicable to be employed in detection of damaged buildings and updating building inventory database. In addition, scale-space presentation of an image can assist the visual interpretation process. Detailed object-based comparison will be developed to classify the damage level of each building or building block. It is possible to obtain the number of damaged buildings by this object-based method. For building inventory database update, we recommend to employ the developed method in extraction of newly constructed buildings in newly developed areas. To extract a newly constructed building in old and dense area, pixel-based is firstly used to locate the potential area and object-based is locally employed afterwards to extract all possible information of this building.

#### ACKNOWLEDGEMENTS

The Quickbird images used in this study are owned by Digital Globe, Inc. The images of Bam, Iran are licensed and provided by Earthquake Engineering Research Institute (EERI), Oakland, California, USA.

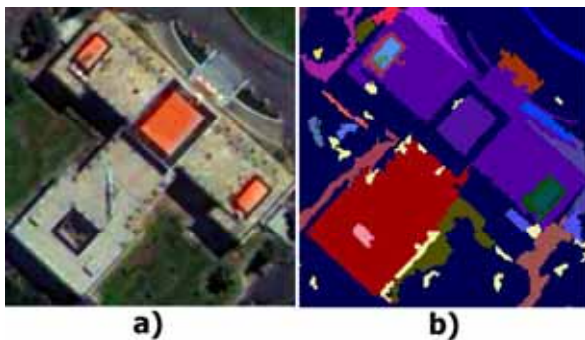


Figure 9. Big and complex structure: a) True color composite and b) extracted result.

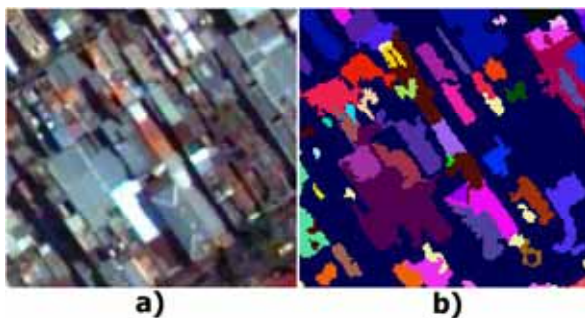


Figure 10. Small residential areas: a) True color composite and b) extract result.

## REFERENCE

- ACTON, S. T. AND MUKHERJEE, D. P., 2000, Scale space classification using area morphology. *IEEE Transactions on Image Processing*, 9 (4), pp. 623-635.
- EGUCHI, R.T., HUYCK, C.K., HOUSHMAND, B., MANSOURI, B., SHINOZUKA, M. YAMAZAKI, F. and MATSUOKA, M., 2000, The Marmara Earthquake: A View from space: The Marmara, Turkey Earthquake of August 17, 1999: Reconnaissance Report. Technical Report MCEER-00-0001: pp. 151-169.
- ESTRADA, M., YAMAZAKI, F., and MATSUOKA, M., 2000, Use of Landsat Images for the Identification of Damage due to the 1999 Kocaeli, Turkey Earthquake. In *Proceedings of 21st Asian Conference on Remote Sensing*, November 2001, Singapore, pp.1185-1190.
- LINDEBERG, T., 1993, Discrete Derivative Approximations with Scale-Space Properties: A Basis for Low-Level Feature Extraction. *Journal of Mathematical Imaging and Vision*, 3 (4), pp. 349-376.
- MATSUOKA, M. and YAMAZAKI, F., 1999, Characteristics of Satellite Images of Damaged Areas due to the 1995 Kobe Earthquake. In *Proceedings of 2nd Conference on the Applications of Remote Sensing and GIS for Disaster Management*, 1999, The George Washington University, CD-ROM.
- MITOMI, H., SAITA, J., MATSUOKA, M. and YAMAZAKI, F., 2001, Automated Damage Detection of Buildings from Aerial Television Images of the 2001 Gujarat, India Earthquake. In *Proceedings of the IEEE 2001 International Geoscience and Remote Sensing Symposium*, IEEE, CD-ROM, 3p.
- PETROVIC, A., DIVORRA ESCODA, O., and VANDERGHEYNST, P., 2004, Multiresolution segmentation of natural images: From linear to non-linear scale-space representations. *IEEE Transactions on Image Processing*, 13 (8), pp. 1104-1114.
- SAITO, K., SPENCE R.J.S., GOING, C., and MARKUS, M., 2004, Using high-resolution satellite images for post-earthquake building damage assessment: a study following the 26 January 2001 Gujarat Earthquake. *Earthquake Spectra*, 20 (1), pp. 145–169.
- SOILLE, P. and PESARESI, M., 2002, Advances in Mathematical Morphology Applied to Geoscience and Remote Sensing. *IEEE Transactions on Geoscience and Remote Sensing*, 40 (9), pp. 2042-2055.
- TOU, J.T. and GONZALEZ, R.C., 1974, *Pattern Recognition Principles*, (Reading, Massachusetts: Addison-Wesley Publishing Company).
- VINCENT, L., 1992, Morphological Area Opening and Closings for Greyscale Images. In *Proceeding NATO Shape in Picture workshop*, Driebergen, The Netherlands, Springer-Verlag, pp. 197-208.
- VINCENT, L., 1994, Fast Grayscale Granulometry Algorithms. In *Proceeding EURASIP Workshop ISMM'94, Mathematical Morphology and its Applications to Image Processing*, Fontainebleau, France, pp. 265-272.
- VU, T. T., MATSUOKA, M., and YAMAZAKI, F., 2005, Detection and Animation of Damage in Bam City Using Very High-resolution Satellite Data, *Earthquake Spectra Special Issue*, 2003 Bam, Iran, Earthquake Reconnaissance report, EERI (in press).
- YAMAZAKI, F., YANO, Y., and MATSUOKA, M., 2005, Visual Damage Interpretation of Buildings in Bam City Using QuickBird Images, *Earthquake Spectra Special Issue*, 2003 Bam, Iran, Earthquake Reconnaissance report, EERI (in press).